

Intrinsic coherence dynamics and phase localization in Aharonov-Bohm Interferometers

Matisse Wei-Yuan Tu,¹ Wei-Min Zhang,^{1,*} and Jinshuang Jin^{1,2}

¹*Department of Physics, National Cheng Kung University, Tainan 70101, Taiwan*

²*Department of Physics, Hangzhou Normal University, Hangzhou 310036, China*

The nonequilibrium real-time dynamics of electron coherence is explored in the quantum transport through the double-dot Aharonov-Bohm interferometers. We solve the exact master equation to find the exact quantum state of the device, from which the changes of the electron coherence through the magnetic flux in the nonequilibrium transport processes is obtained explicitly. We find that the relative phase between the two charge states of the double dot localizes to $\frac{\pi}{2}$ or $-\frac{\pi}{2}$ for all different magnetic flux. This nontrivial phase localization process can be manifested in the measurable occupation numbers.

PACS numbers: 03.65.Yz, 73.63.Kv, 73.40.Gk

Introduction.— Quantum coherence and quantum transport in mesoscopic electronic systems has attracted much attention due to recent achievements in quantum technology. Controlling quantum coherence in various quantum devices is essential to their functioning. Especially in a ring structured Aharonov-Bohm (AB) interferometer where electron interference can be tuned by an externally applied magnetic flux, a great amount of efforts has been made to investigate its coherence transport properties, mostly in the steady limit [1–12]. Alternatively we address here the real-time dynamics of building electron coherence and then the subsequent evolution of the intrinsic coherence in a two-terminal AB interferometer with two quantum dots (QDs).

Coherence of electron transport through an AB interferometer has long been characterized via conductance oscillation in magnetic fields [1–3]. Factors influencing AB oscillations include “which path detection” [1, 4, 5], electron-electron interaction [6, 7, 9] and inelastic scattering with phonons [10], etc. Extracting the transmission phase from AB oscillations has always been the focus (see [11, 12] and references there in) since it may contain information about coherence of electron transport other than the interference by the AB phase. For a double dot AB interferometer, what most intuitively depicts the electron coherence other than AB interference is the relative phase between the two dot charge states. This intrinsic phase is generally entangled with the AB phase and its fundamental dynamics has not been well understood so far. However, the dynamics of this intrinsic phase is important for manipulating quantum coherence in the application of quantum information processing. Therefore in this Letter we shall directly study the nonequilibrium electron dynamics to examine the effects of the magnetic flux on the relative phase.

To explore the intrinsic coherence dynamics, we solve exactly the time evolution of the electron charge states in the double dot AB interferometer. We found that although different values of magnetic flux will induce different relative phases initially, they will eventually be

localized to $\pi/2$ or $-\pi/2$. Remarkably, this phase localization dynamics is reflected in the occupation number rather than the transport current. For the latter, its magnetic flux dependence has been extensively employed in characterizing the coherence of electron transport.

Reduced density matrix and exact master equation.— The system under consideration is described by the Hamiltonian consisting of three parts, $\mathcal{H} = \mathcal{H}_s + \mathcal{H}_{\text{lead}} + \mathcal{H}_c$. $\mathcal{H}_s = \sum_{ij} E_{ij} a_i^\dagger a_j$ where $i, j = 1, 2$ is the Hamiltonian of the interferometer, with a_i (a_i^\dagger) destroying (creating) an electron on dot i . The lead Hamiltonian is $\mathcal{H}_{\text{lead}} = \sum_{\alpha\mathbf{k}} \epsilon_{\alpha\mathbf{k}} c_{\alpha\mathbf{k}}^\dagger c_{\alpha\mathbf{k}}$, where $\alpha = L$ or R and $c_{\alpha\mathbf{k}}$, $c_{\alpha\mathbf{k}}^\dagger$ the electronic operators of the leads, and

$$\mathcal{H}_c = \sum_{j\mathbf{k}} [V_{jL\mathbf{k}} e^{i\phi_{jL}} a_j^\dagger c_{L\mathbf{k}} + V_{jR\mathbf{k}} e^{i\phi_{jR}} c_{R\mathbf{k}}^\dagger a_j + \text{H.c.}] \quad (1)$$

describes the coupling between the dots and the leads. In Eq. (1), $\phi_{j\alpha}$ are the AB phase factors due to the AB flux Φ such that $\phi_{1L} - \phi_{2L} + \phi_{1R} - \phi_{2R} = \phi \equiv 2\pi\Phi/\Phi_0$ with Φ_0 being the flux quantum. To single out the effects of the threading magnetic flux, we will not include explicitly the electron-electron interaction here.

Coherence between the two electron charge states of the double dot is embedded in the reduced density matrix ρ of the double dot system, which can be obtained by tracing over the lead electrons from the total reduced density matrix $\rho_{\text{tot}}(t) = e^{-i\mathcal{H}(t-t_0)} \rho_{\text{tot}}(t_0) e^{i\mathcal{H}(t-t_0)}$. The (exact) equation of motion for ρ has been derived in Ref. [13, 14]. Assuming that initially, at $t = t_0$, the dots are uncorrelated with the leads [15], then

$$\begin{aligned} \dot{\rho} = & -i[\mathcal{H}'_S(t), \rho(t)] \\ & + \sum_{ij} \left\{ \gamma_{ij}(t) (2a_j \rho(t) a_i^\dagger - a_i^\dagger a_j \rho(t) - \rho(t) a_i^\dagger a_j) \right. \\ & \left. + \tilde{\gamma}_{ij}(t) (a_j \rho(t) a_i^\dagger - a_i^\dagger \rho(t) a_j - a_i^\dagger a_j \rho(t) + \rho(t) a_j a_i^\dagger) \right\}. \end{aligned} \quad (2)$$

Here, $\mathcal{H}'_S(t) = \sum_{ij} \epsilon'_{ij}(t) a_i^\dagger a_j$ is the renormalized Hamiltonian of the double dot; ϵ' and all other time-dependent

coefficients in Eq. (2) are given by $\epsilon'_{ij}(t) - i\gamma_{ij}(t) = i[\dot{\mathbf{u}}\mathbf{u}^{-1}]_{ij}$, $\tilde{\gamma}_{ij}(t) = [\dot{\mathbf{u}}\mathbf{u}^{-1}\mathbf{v} + \text{H.c.} - \dot{\mathbf{v}}]_{ij}$, where the matrix functions \mathbf{u} and \mathbf{v} obey the following equations [16]

$$\dot{\mathbf{u}}(\tau) + i\mathbf{E}\mathbf{u}(\tau) + \int_{t_0}^{\tau} d\tau' \mathbf{g}(\tau - \tau')\mathbf{u}(\tau') = 0, \quad (3a)$$

$$\begin{aligned} \dot{\mathbf{v}}(\tau) + i\mathbf{E}\mathbf{v}(\tau) + \int_{t_0}^{\tau} d\tau' \mathbf{g}(\tau - \tau')\mathbf{v}(\tau') \\ = \int_{t_0}^t d\tau' \tilde{\mathbf{g}}(\tau - \tau')\mathbf{u}^\dagger(t - \tau' + t_0), \end{aligned} \quad (3b)$$

with the initial conditions $\mathbf{u}(t_0) = I$, $\mathbf{v}(t_0) = 0$. In Eq. (3), \mathbf{E} is the 2×2 energy matrix of the double-dot, \mathbf{g} and $\tilde{\mathbf{g}}$ are the temporal correlation functions resulted from the couplings to the leads via the spectral density,

$$\Gamma_{\alpha ij}(\omega) = 2\pi \sum_{\mathbf{k} \in \alpha} V_{i\alpha\mathbf{k}} V_{j\alpha\mathbf{k}} e^{i(\phi_{i\alpha} - \phi_{j\alpha})} \delta(\omega - \epsilon_{\alpha\mathbf{k}}), \quad (4)$$

such that [13]: $\mathbf{g}(\tau) = \sum_{\alpha=L,R} \int \frac{d\omega}{2\pi} e^{-i\omega\tau} \Gamma_{\alpha}(\omega)$ and $\tilde{\mathbf{g}}(\tau) = \sum_{\alpha=L,R} \int \frac{d\omega}{2\pi} f_{\alpha}(\omega) e^{-i\omega\tau} \Gamma_{\alpha}(\omega)$, where $f_{\alpha}(\omega) = (\exp[(\omega - \mu_{\alpha})/k_B T] + 1)^{-1}$ is the initial Fermi distribution for the electron reservoir (lead) $\alpha = L, R$.

Exact solution of the master equation.— To monitor the formation of coherence in the transport process, we prepare the double dot with the empty state $|0\rangle$ at $t = t_0$. We denote the singly occupied states by $|1\rangle$ and $|2\rangle$ referring to occupation of the first dot and the second dot, respectively, as the two charge state basis. And the double occupancy is denoted by $|3\rangle$. From the master equation (2) with the above preparation, the reduced density matrix becomes

$$\rho(t) = \begin{pmatrix} \rho_{00}(t) & 0 & 0 & 0 \\ 0 & v_{11}(t) - \rho_{33}(t) & v_{12}(t) & 0 \\ 0 & v_{21}(t) & v_{22}(t) - \rho_{33}(t) & 0 \\ 0 & 0 & 0 & \rho_{33}(t) \end{pmatrix}, \quad (5)$$

where the dynamics of the relative phase between the two charge states is given explicitly by the off-diagonal matrix element $\rho_{12}(t) = v_{12}(t)$, while $\rho_{00}(t) = \det[I - \mathbf{v}(t)]$ and $\rho_{33}(t) = \det \mathbf{v}(t)$ determine the leakage effect and the double occupation, respectively, and $\rho_{ii}(t) = v_{ii}(t) - \rho_{33}(t)$ ($i = 1, 2$) is the probability of each singly occupied charge state. It is obvious that the total probability is conserved: $\text{tr}\rho(t) = 1$. The full reduced density matrix is thus determined from $\mathbf{v}(t)$ which has a general solution from Eq. (3b),

$$\mathbf{v}(t) = \int \frac{d\omega}{2\pi} \mathbf{u}(t, \omega) \sum_{\alpha} f_{\alpha}(\omega) \Gamma_{\alpha}(\omega) \mathbf{u}^\dagger(t, \omega), \quad (6)$$

where $\mathbf{u}(t, \omega) \equiv \int_{t_0}^t d\tau e^{i\omega(t-\tau)} \mathbf{u}(t - \tau + t_0)$. It is then sufficient to solve the first line of Eq. (3) for a full understanding of the intrinsic coherence dynamics.

As being widely studied in the literature, with a degenerate double dot given by the Hamiltonian $\mathcal{H}_s = \sum_i E a_i^\dagger a_i$ and an equal coupling $\Gamma_L = \Gamma_R = \Gamma/2$ in the white band limit, we can well suppress the relaxation dynamics and exclusively focus on the relative phase dynamics. Also, as a convention, we choose the gauge $\phi_{1L} - \phi_{2L} = \phi_{1R} - \phi_{2R} = \phi/2$. These considerations lead to $\Gamma_{L,R} = \frac{\Gamma}{2} \begin{pmatrix} 1 & e^{\pm i\phi/2} \\ e^{\mp i\phi/2} & 1 \end{pmatrix}$. One can easily obtain from Eq. (3a), by taking $t_0 = 0$,

$$\mathbf{u}(t) = e^{-(iE + \frac{\Gamma}{2})t} \left(\cosh \frac{\Gamma\phi t}{2} - \sigma_x S(\phi) \sinh \frac{\Gamma\phi t}{2} \right), \quad (7)$$

where $\Gamma_{\phi} = \Gamma |\cos(\phi/2)|$ and $S(\phi) = \frac{\cos(\phi/2)}{|\cos(\phi/2)|}$. Straightforwardly one can also find from Eq. (6)

$$\mathbf{v}(t) = v_0(t)I + v_x(t)\sigma_x + v_y(t)\sigma_y + v_z(t)\sigma_z, \quad (8)$$

where $v_0(t) = A_+(t) + A_-(t)$ and $\{v_x(t), v_y(t), v_z(t)\} = \{S(\phi)(A_+(t) - A_-(t)), -\text{Re}B(t), S(\phi)\text{Im}B(t)\}$ with

$$\begin{aligned} A_{\pm}(t) &= \frac{\Gamma}{4} (1 \pm |\cos \frac{\phi}{2}|) \int \frac{d\omega}{2\pi} [f_L(\omega) + f_R(\omega)] |u_{\pm}(t, \omega)|^2, \\ B(t) &= \frac{\Gamma}{2} \sin \frac{\phi}{2} \int \frac{d\omega}{2\pi} [f_L(\omega) - f_R(\omega)] u_+(t, \omega) u_-^*(t, \omega), \end{aligned} \quad (9)$$

$u_{\pm}(t, \omega) = \frac{e^{i(\omega-E)t - \frac{1}{2}(\Gamma \pm \Gamma_{\phi})t} - 1}{i(\omega-E) - \frac{1}{2}(\Gamma \pm \Gamma_{\phi})}$. The notation σ_i with $i = x, y, z$ denotes the Pauli matrices.

Phase localization.— The electron coherence dynamics is embedded in the two charge state density matrix [the central block matrix in Eq. (5)] which can be rewritten as

$$\rho_{\mathbf{q}}(t) = \frac{1}{2} [I + \mathbf{r}(t) \cdot \boldsymbol{\sigma}] - \frac{\rho_{00}(t) + \rho_{33}(t)}{2} I, \quad (10)$$

where $\mathbf{r}(t) = 2\{v_x(t), v_y(t), v_z(t)\}$ is the polarization vector of the two charge states, and $\rho_{00}(t) + \rho_{33}(t)$ clearly shows the leakage effect. To exclusively study the coherence between the two charge states, we shall apply a bias, $\mu_L - E = E - \mu_R$ such that the two dots would be equally occupied, $\rho_{11}(t) = \rho_{22}(t)$, i.e. $r_z(t) = 0$ because $\text{Im}(u_+(t, \omega)u_-^*(t, \omega))$ is antisymmetric in ω with respect to E . The polarization vector then is fully specified by $r_x(t) = 2\text{Re}\rho_{12}(t) = 2v_x(t)$ and $r_y(t) = -2\text{Im}\rho_{12} = 2v_y(t)$, which shows purely the dynamics of coherence between the two charge states through the relative phase $\varphi(t)$, defined explicitly by

$$\rho_{12}(t) = |\rho_{12}(t)| e^{i\varphi(t)} = \frac{1}{2} [r_x(t) - ir_y(t)]. \quad (11)$$

Fig. 1 plots the time evolutions ρ_{12} . At $\phi = 2m\pi$ where m is an arbitrary integer, $\text{Re}\rho_{12}$ soon grows to stable values $\pm 1/4$ (with a time scale $\sim 1/\Gamma$) and $\text{Im}\rho_{12}$ keeps zero, which locks the relative phase φ to 0 or π . However,

when $\phi \neq 2m\pi$, $\text{Re}\rho_{12}$ also grows to a maximal value (coherence building) with the same time scale and then decays to zero at a flux dependent rate $\Gamma(1 - |\cos(\phi/2)|)$. Eventually all the different relative phases are localized to $\pi/2$ or $-\pi/2$. Fig. 2 further visualizes this process. At short time $t = 2/\Gamma$, the direction of $\mathbf{r}(t)$ sweeps over the whole plane, which shows all kinds of relative phases between the two charge states induced by different values of the magnetic fluxes ($-2\pi \leq \phi \leq 2\pi$) [see Fig. 2(a)], as a process of building coherence from the initial empty state. These different values (corresponding to different relative phases) then move toward the y axis as time goes on, except for the points $\phi = (0, \pm 2\pi)$, see Fig. 2(b) and (c), and finally reside on it as the asymptotic limit shown in Fig. 2(d) as the phase localization.

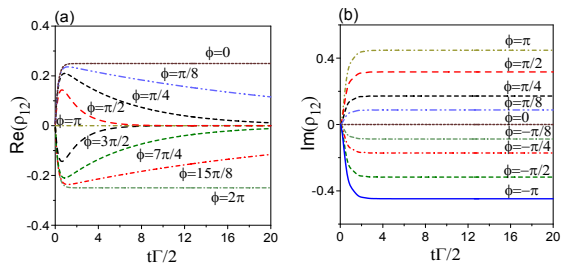


FIG. 1: The time evolution of ρ_{12} . (a) $\text{Re}\rho_{12}$ is plotted for ϕ from 0 to 2π since it is antisymmetric to $\phi = \pi$. (b) $\text{Im}\rho_{12}$ is plotted for ϕ from $-\pi$ to π and it is antisymmetric to $\phi = 0$. Here we take $\mu_L - \mu_R = 6\Gamma$ at temperature $k_B T = \Gamma/5$.

The period of the two charge states in ϕ is 4π as a result of the intrinsic geometry of a two-level system. Though the relative phase is constant over the whole range of $-2\pi < \phi < 2\pi$, except for $\phi = 0$, the degree of interference $|\rho_{12}|$ continuously changes with the flux as well as the bias. At zero bias, $|\rho_{12}|$ becomes zero in the steady limit, as a result of the statistical equilibrium. Therefore, the nonzero bias is crucial to manifest the above phase localization. We should also point out that this phase localization over the magnetic flux is gauge independent.

To observe such process, we examine two measurable quantities, the transport current passing through the double dot and the occupation number in the two dots. The former, usually derived from the nonequilibrium Green function technique [17], can also be obtained within our theory (see the explicit derivation in [14] and the result is consistent with [17]):

$$I(t) = \frac{\Gamma}{2} \text{Re} \int \frac{d\omega}{2\pi} (f_L(\omega) - f_R(\omega)) \left\{ (1 + |\cos \frac{\phi}{2}|) u_+(t, \omega) + (1 - |\cos \frac{\phi}{2}|) u_-(t, \omega) - \Gamma \sin^2 \frac{\phi}{2} u_+(t, \omega) u_-^*(t, \omega) \right\}. \quad (12)$$

The last term in the above current expression is indeed proportional to $\text{Im}\rho_{12}$. The result is plotted in Fig. 3(a). As one can see, the current always oscillates smoothly in

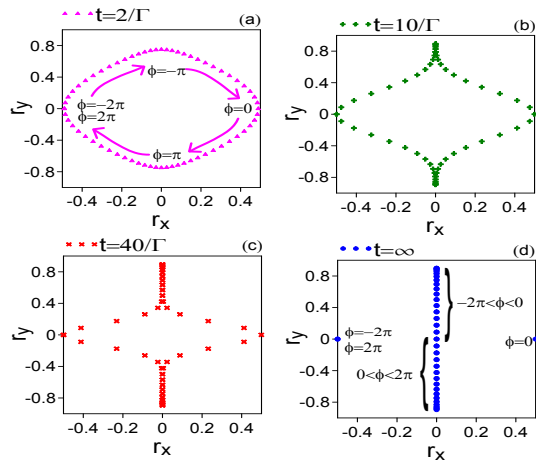


FIG. 2: Distribution of (r_x, r_y) among different values of ϕ from -2π to 2π at different times. The parameters are the same as that used in Fig. 1. Note that changing the direction of the magnetic flux $\phi \rightarrow -\phi$, one flips the sign of r_y while the sign of r_x is flipped around $\phi = \pm\pi$ as seen also in Fig. 1.

ϕ (showing the AB oscillation alone). The sharp transitions across $\phi = 2m\pi$ and the invariance of the relative phase over the whole range of flux, as the main features of phase localization, do not be seen in the transport current. However, we find that the occupation number, $n_i = \rho_{ii} + \rho_{33}$ with $i = 1, 2$, which depends on $\text{Re}\rho_{12}$ via $\dot{n}_i(t) = -\Gamma n_i(t) - \Gamma \cos(\phi/2) \text{Re}\rho_{12}(t) - \tilde{\gamma}_{ii}(t)$, does display the features of the phase localization discussed above. The occupation number initially oscillates smoothly in ϕ , and in the steady limit,

$$n_i(t \rightarrow \infty) = \frac{1}{2} - \cos(\phi/2) \text{Re}\rho_{12}(t \rightarrow \infty). \quad (13)$$

As shown in Fig. 3(b), the phase localization to $\pi/2$ and $-\pi/2$ [as a result of $\text{Re}\rho_{12}(t \rightarrow \infty) = 0$] are explicitly manifested by the invariance of $n_i(t \rightarrow \infty) = 1/2$ over the whole range of the flux, except for $\phi = 2m\pi$ ($m = 0, \pm 1$). At $\phi = 2m\pi$, sharp change of $\text{Re}\rho_{12}$ to $\pm 1/4$ is also manifested as a sharp reduction of the occupation number n_i from $1/2$ to $1/4$.

Fig. 3(c) and (d) further reveals the underlying picture of the phase localization. It shows that ρ_{11} only contains the AB oscillation (oscillates in ϕ smoothly), just like the transport current I does [see Fig. 3(a) and (c)]. The asymptotic constant occupation $1/2$ (manifesting the phase localization) for any flux $\phi \neq 2m\pi$ is contributed mainly from the double occupation ρ_{33} . Furthermore, the sharp reduction of occupation number from $1/2$ to $1/4$ is indeed rooted in the vanishing double occupancy at $\phi = 2m\pi$. As we know, strong inter-dot Coulomb repulsion may prohibit double occupancy regardless of the flux. Phase localization then might not be expected in this case. However, the parameters of the system can be well tuned to make the inter-dot Coulomb

repulsion become unimportant so that the phase localization can always be manifested.

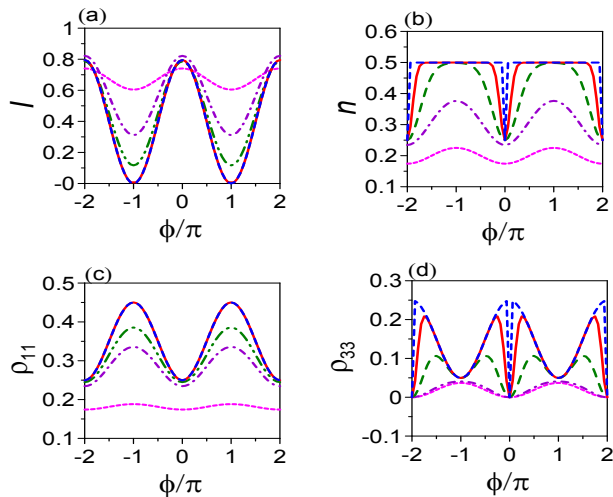


FIG. 3: The dependencies of the current I , the occupation number $n = n_1 = n_2 = \rho_{11} + \rho_{33}$, single occupancy probability ρ_{11} and double occupancy ρ_{33} on ϕ are examined at various times (the line styles are $t = 0.6/\Gamma$: pink ultrashort dashed, $t = 1.4/\Gamma$: purple dash-dot, $t = 2/\Gamma$: green dash-dot-dot, $t = 6/\Gamma$: green long dashed, $t = 40/\Gamma$: red solid and $t = \infty$: blue short dashed). Both ρ_{11} and ρ_{33} oscillate in flux in such a way that n is kept as a constant for $\phi \neq 2m\pi$.

The above discussion has centered on degenerate double dot. Practically there is no perfect degenerate double dot. However, we find that slightly splitting the degeneracy only slightly deviates the result of phase localization while the main property is still well preserved. As one can see from Fig. 4(a), $r_x = 2\text{Re}\rho_{12}$ is lifted a little bit from zero for the flux values near $2m\pi$. Similar signals on the occupation number can also be seen reflecting such a slight deviation for the phase localization, as shown in Fig. 4(b). Comparing to the transport current, the electron occupation in each dot is easier to be measured in experiments using, for example, SET or QPC [18], this phenomenon can be well observed experimentally.

Conclusion.— We have directly studied the dynamical effects of the magnetic flux on the relative phase between two electron charge states in a double dot AB interferometer by exactly solving the nonequilibrium electron dynamics of the system. We found that the flux dependence of the relative phase characterizing the intrinsic electron coherence lead to a phase localization through the nonequilibrium electron transport over the whole range of flux except for the points $\phi = 2m\pi$ ($m = 0, \pm 1$). We also found that such distinguished dynamics of phase localization is manifested in the occupation number which is expected to be measurable in experiments.

We would like to thank Amnon Aharony and Ora Entin-Wohlman for the extensive and fruitful discussions to the problems addressed in this paper and also for help-

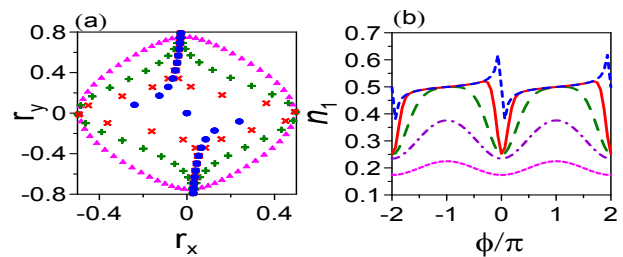


FIG. 4: The distribution of the polarization (r_x, r_y) and the occupation number n_1 deviated away from the degenerate double dot, with energy level difference $E_1 - E_2 = 2.5\%\Gamma$, are plotted in (a) and (b), respectively, at various times. The symbols and the corresponding time values used in (a) are the same as that used in Fig. 2. The different curves corresponding to various times in (b) are the same as that in Fig. 3(b). n_2 is almost the same as n_1 since the deviation is small.

ing to improve the presentation of the manuscript. This work is supported by the National Science Council of ROC under Contract No. NSC-99-2112-M-006-008-MY3. We also thank the support from National Center for Theoretical Science of Taiwan.

* Electronic address: wzhang@mail.ncku.edu.tw

- [1] A. Yacoby, M. Heiblum, D. Mahalu, and H. Shtrikman Phys. Rev. Lett. **74**, 4047 (1995); R. Schuster, E. Buks, M. Heiblum, D. Mahalu, V. Umansky, and H. Shtrikman, Nature **385**, 417 (1997).
- [2] Y. Imry, *Introduction to Mesoscopic Physics*, 2nd ed. (Oxford University Press, Oxford, 2002).
- [3] A. C. Bleszynski-Jayich, W. E. Shanks, B. Peaudecerf, E. Ginossar, F. von Oppen, L. Glazman, and J. G. E. Harris, Science **326**, 272 (2009).
- [4] Y. Levinson, Europhys. Lett. **39**, 299 (1997).
- [5] I. L. Aleiner, N. S. Wingreen, and Y. Meir, Phys. Rev. Lett. **79**, 3740 (1997).
- [6] A. Stern, Y. Aharonov, and Y. Imry, Phys. Rev. A **41**, 3436 (1990).
- [7] G. Hackenbroich, Phys. Rep. **343**, 463 (2001), and references therein.
- [8] B. Kubala and J. König, Phys. Rev. B **65**, 245301(2002).
- [9] J. König and Y. Gefen, Phys. Rev. Lett. **86**, 3855 (2001); Z. T. Jiang, Q. F. Sun, X. C. Xie and Y. Wang, Phys. Rev. Lett. **93**, 076802 (2004).
- [10] M. Sigrist, T. Ihn, K. Ensslin, D. Loss, M. Reinwald, W. Wegscheider, Phys. Rev. Lett. **96**, 036804 (2006).
- [11] O. Entin-Wohlman, A. Aharony, Y. Imry, Y. Levinson, and A. Schiller, Phys. Rev. Lett. **88**, 166801 (2002)
- [12] V. I. Puller and Y. Meir Phys. Rev. Lett. **104**, 256801 (2010)
- [13] M. W. Y. Tu and W. M. Zhang, Phys. Rev. B **78**, 235311 (2008); M. W. Y. Tu, M. T. Lee, and W. M. Zhang, Quantum Inf. Processing (Springer) **8**, 631 (2009).
- [14] J. S. Jin, M. W. Y. Tu, W. M. Zhang, and Y. J. Yan, New J. Phys. **12**, 083013 (2010).
- [15] A. J. Leggett, S. Chakravarty, A. T. Dorsey, M.P. Fisher, A. Garg, and W. Zwerger, Rev. Mod. Phys. **59**, 1 (1987).

- [16] It can be shown [14] that \mathbf{u} and \mathbf{v} are directly related to the retarded and lesser Green functions, respectively, of the nonequilibrium Keldysh scheme [17].
- [17] H. Haug and A.-P. Jauho, *Quantum Kinetics in Transport and Optics of Semiconductors*, Springer Series in Solid-State Sciences **123**, 2nd Ed. (Springer-Verlag, Berlin, 2008).
- [18] M. H. Devoret and R. J. Schoelkopf, *Nature*, **406**, 1039 (2000); T. Fujisawa, T. Hayashi, and S. Sasaki, *Rep. Prog. Phys.* **69**, 759 (2006).